Tetrahedron 67 (2011) 8717–8723

Contents lists available at SciVerse ScienceDirect

Tetrahedron

journal homepage: www.elsevier.com/locate/tet

Unexpected highly selective fluorescence 'turn-on' and ratiometric detection of Hg^{2+} based on fluorescein platform

Yi-Bin Ruan, Juan Xie *

PPSM, Institut d'Alembert, ENS Cachan, CNRS, 61 av President Wilson, F-94230 Cachan, France

ARTICLE INFO

Article history:
Received 11 July 2011
Received in revised form 30 August 2011
Accepted 9 September 2011
Available online 14 September 2011

Keywords:
Chemosensor
Methylated fluorescein
Hg^{2+}
Ratiometric detection

ABSTRACT

Methylated fluorescein **1** was explored for fluorescence 'turn-on' and ratiometric detection of Hg^{2+} in THF and CH_2Cl_2/MeOH (v/v=9:1), respectively, with unexpected high selectivity. In the presence of Hg^{2+}, characteristic structured absorption band of **1** diminished and a new sharp band appeared at 445 nm. Meanwhile a blue shifted and enhanced emission was observed. The ratio of the fluorescence intensity at 559 and 478 nm increased linearly with [Hg^{2+}], and solution color changing from yellow to cyan under irradiation at 365 nm in CH_2Cl_2/MeOH. Job plot indicated a 1:1 stoichiometry for **1**–Hg^{2+} complex in solution. ^{1}H NMR titration and IR spectra suggested the coordination of carbonyl group in xanthene moiety to Hg^{2+}, affording its spectral behavior. Compound **2** bearing two triazolyl amino esters in place of methyl group showed quite similar behavior to Hg^{2+}, which indicated that substituents did not interfere with the specific binding behavior of fluorescein platform. Our work presents a new way to explore xanthene dyes as new chemosensors by modulating electron density on the xanthene ring through non-covalent interactions with carbonyl group.

1. Introduction

Mercury as one of the most hazardous metal ions is a widespread pollutant. Excessive exposure to mercury compounds causes serious and destructive effects on human health, such as heart diseases and neurological problems.[1] Fluorescent chemosensors have attracted considerable interest for decades due to their intrinsic advantages in terms of simplicity, selectivity, sensitivity, and biological applications. To date, important progress has been achieved by developing turn-on fluorescent analyses of mercury,[2] which are mainly based on small organic fluorophores,[3] fluorescent conjugated polymers[4] and biomolecules.[5] However, most of them require sophisticated organic synthesis and/or high cost, which limit their practical applications. Ratiometric methods represent an alternative approach by comparison of the fluorescence intensity at two different wavelengths upon addition of analytes. Although this method shows great advantages in its dynamic range and has a built-in correction for environmental effects, there are still few reports of detection of Hg^{2+} based on fluorescent ratiometric signaling transduction.[6]

Fluorescein derivatives have been extensively utilized in biological applications due to their excellent photophysical properties.[7] Appropriate modification of fluorescein either on xanthene or benzoic acid moiety can result in plenty of interesting properties for the further applications.[8] Many of them have been used as fluorescent chemosensors for monitoring pH,[9] metal ions,[10] anion,[11] and other biologically important targets.[12] At present there are mainly three approaches proposed for the sensory mechanisms: (a) spirolactone ring opening; (b) photoinduced electron transfer (PET); (c) modulation on hydroxyl/carbonyl group.[10i,14] Lippard's group has pioneered in the field of developing NO, Zn^{2+}, and Hg^{2+} 'turn-on' fluorescent chemosensors through suppressing the PET process from electron donating nitrogen atom to various fluorescein cores.[10a–e,12] As a continuing interest in fluorescent chemosensors for metal ions,[10j,13] we turn our attention to modulation of hydroxyl/carbonyl group of xanthene moiety for sensory applications as its photophysical properties can be easily modulated by changing chemical environment based on covalent and/or non-covalent interactions (Scheme 1). For example, alkylation of hydroxyl group significantly reduced the fluorescence efficiency.[14] In addition, fluorescein derivatives display quite different spectral behavior in solutions with different hydrogen bonding ability and/or polarity.[14–16] Based on the cleavage of C–O ether bond, many 'turn-on' fluorescent chemosensors for different analytes have been developed.[15] To date, little attention has been paid to metal coordination interaction with carbonyl group of xanthene moiety, which is stronger than hydrogen bond while weaker than covalent bond. According to the literatures, hydrogen bonding interaction usually increases fluorescence quantum yield of fluorescein derivatives;[16] while formation of C–O ether bond usually induces

* Corresponding author. Tel.: +33 1 47405586; fax: +33 1 47402454; e-mail address: joanne.xie@ens-cachan.fr (J. Xie).

0040-4020/$ – see front matter © 2011 Elsevier Ltd. All rights reserved.
doi:10.1016/j.tet.2011.09.028

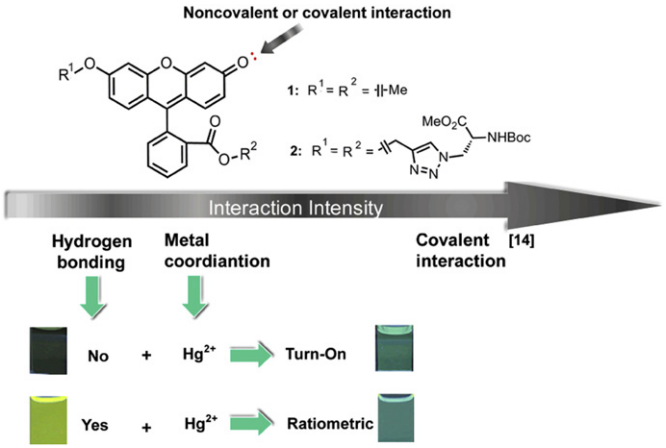

Scheme 1. Schematic illustration of our sensing approach.

fluorescence quenching.[14] When the carbonyl group in xanthene moiety is a binding site for metal ions, how metal coordination interaction will affect spectral properties of the xanthene moiety attracts our interest. For this proposal, we used compounds **1** and **2** to investigate metal coordination effect on spectral properties of xanthene fluorophores (Scheme 1). Out of expectation, we found that compound **1** with carbonyl group as the single binding site could selectively response to Hg^{2+} in THF in 'turn-on' fluorescence manner. Furthermore, we also developed ratiometric detection of Hg^{2+} in CH_2Cl_2/CH_3OH (v/v=9:1) through utilization of both intermolecular hydrogen bonding and metal coordination interactions.

2. Results and discussion

2.1. Synthesis

Methylated fluorescein **1** was synthesized by a two-step reaction according to the literature (Scheme 2).[17] Compound **2**, where the two methyl groups were replaced by two triazolyl amino esters was prepared previously by Cu(I)-catalyzed Huisgen cycloaddition reaction.[18]

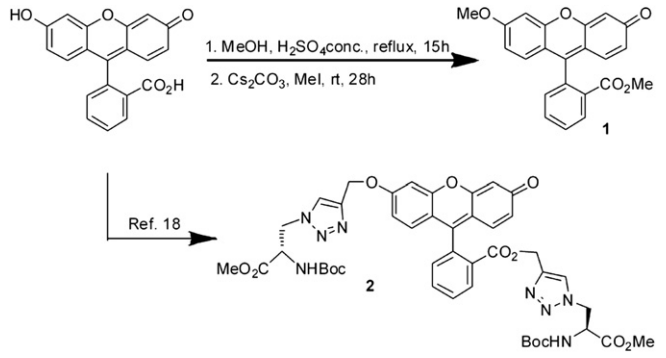

Scheme 2. Synthesis of compounds **1** and **2**.

2.2. Photophysical properties

We first investigated solvatochromic effect of **1** in selected organic solvents. As presented in Fig. 1 and Table 1, compound **1** exhibited structured absorption bands at ca. 432, 458, 488 nm and emission bands at 518–562 nm without remarkable wavelength shift (less than 13 nm) in different organic solvents, corresponding

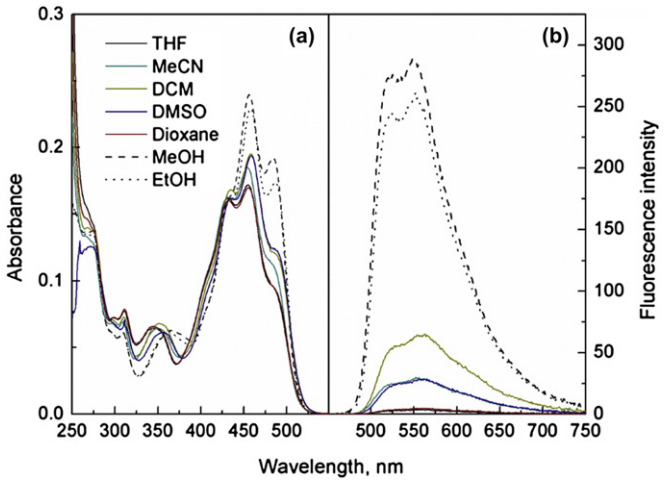

Fig. 1. Absorption (a) and fluorescence (b) spectra of **1** in various solvents; excitation wavelengths corresponding to the maximum absorption band, [**1**]=10 μM.

Table 1
Photophysical data of **1** and **2** in different organic solvents

Compounds	Solvents	λ^A_{max} [nm]	ε_{00} [10^4 L mol^{-1} cm^{-1}]	λ^F_{max} [nm]	Φ_F[a] %
1	Dioxane	432, 456, 487	1.7, 1.8, 1.0	518, 562	0.6
	DMSO	433, 458, 488	1.7, 2.1, 1.3	527, 562	4.0
	CH_2Cl_2	434, 458, 488	1.8, 2.1, 1.3	529, 561	8.5
	MeCN	432, 454, 485	1.7, 1.9, 1.2	520, 553	3.6
	THF	431, 455, 486	1.7, 1.8, 1.0	518, 562	0.5
	EtOH	433, 458, 487	1.7, 2.5, 1.9	523, 549	27.3
	MeOH	432, 456, 484	1.7, 2.5, 2.0	523, 549	27.2
2	Dioxane	433, 456, 488	1.8, 2.2, 1.4	526, 565	1.8
	DMSO	438, 460, 489	1.9, 2.2, 1.4	524, 559	4.2
	CH_2Cl_2	434, 458, 490	1.9, 2.2, 1.3	528, 561	8.1
	MeCN	432, 456, 486	1.8, 2.1, 1.3	522, 557	4.6
	THF	433, 456, 488	1.8, 1.9, 1.1	526, 565	1.1
	EtOH	434, 459, 489	1.8, 2.5, 1.9	523, 553	24.1
	MeOH	433, 457, 486	1.8, 2.6, 2.0	523, 553	24.8

[a] Coumarin 153 was used as the standard in EtOH[20].

to characteristics of the quinoid form of fluorescein. In aprotic solvents, only slight differences in the absorptivity and fluorescence quantum yields could be observed (Fig. 1 and Table 1), showing no direct connection between spectral properties and solvent polarity. It is worthy of notice that stronger absorptivity at 487 nm and higher fluorescence intensity in protic solvents like EtOH and MeOH were observed. Moreover, fluorescence quantum yields of **1** in protic solvents are higher than in non-protic ones, which are consistent with the results mentioned above (Table 1). This can be explained by intermolecular hydrogen bonding interaction between **1** and protic solvents, which could reduce the interconversion in the excited states and consequently improved the emission efficiency. Evidences from Martin's group demonstrated that higher the solvent hydrogen bond donating power was, larger the blue shift of the absorption and fluorescence spectra and enhancement of fluorescence quantum yields.[16]

2.3. Spectral behavior of 1 toward metal ions

To investigate metal binding ability of **1** and effect of metal coordination interaction on its photophysical properties, we tested spectral response of **1** to various metal ions such as Hg^{2+} (40 μM), Li^+, Na^+, K^+, Ag^+, Ba^{2+}, Cd^{2+}, Co^{2+}, Cu^{2+}, Fe^{2+}, Mg^{2+}, Mn^{2+}, Ni^{2+}, Pb^{2+}, and Zn^{2+} at 80 μM in THF. To our surprise, only the addition of Hg^{2+} resulted in blue shift of the absorption and emission bands, concomitantly with remarkable fluorescence enhancement (Fig. 2).

Other tested metal ions showed almost no influence. The selectivity of **1** to Hg^{2+} was further confirmed by the presence of interfering metal ions. As shown in Fig. 3, except Ag^{+}, the coexisted metal ions (1 equiv) produced no influence on the spectral response of **1** to Hg^{2+} in THF. These results demonstrated that compound **1**, containing carbonyl group as the single binding site, exhibited selective response to Hg^{2+} in THF.

Spectral titrations were then carried out to get further insight into the binding process of **1** to Hg^{2+} in THF. As shown in Fig. 4 (top), upon addition of increasing [Hg^{2+}], absorption band of **1** at 490 nm decreased, concomitantly with appearance of a new narrow band at 445 nm. Well-defined isosbestic points were observed at 462 and 403 nm, indicating equilibrium of the complexation process. Job's plot, which showed the maximum at 0.5 of the fraction demonstrated that the binding stoichiometry between **1** and Hg^{2+} is 1:1 (Fig. 5). The binding constant in the ground state was determined to be 3.55×10^{5} M^{-1} by using non-linear regression analysis based on 1:1 binding ratio (Fig. 4 (top)). Meanwhile, addition of Hg^{2+} induced a blue shift of the emission band from 560 to 489 nm, with remarkably enhanced fluorescence intensity (ca. 13 folds) (Fig. 4 (bottom)) and solution color changing from dark to cyan under UV irradiation at 365 nm. The association constant in the excited state was determined to be 3.14×10^{5} M^{-1}. The binding constant of 10^{4}–10^{5} M^{-1} for a carbonyl-Hg^{2+} interaction in aqueous or acetone solution has been reported by Avirah et al.[19] The detection limit of the probe in THF was 39 nM (3σ/k) for Hg^{2+}. However, when it was performed in aqueous solution (V_{H_2O}/V_{THF} = 5 : 95), quite little influence was observed on the spectral properties of **1** even in the presence of 4.0 equiv of Hg^{2+}, which could be attributed to strong hydration of Hg^{2+} inhibiting its complexation with the receptor (Fig. S1).

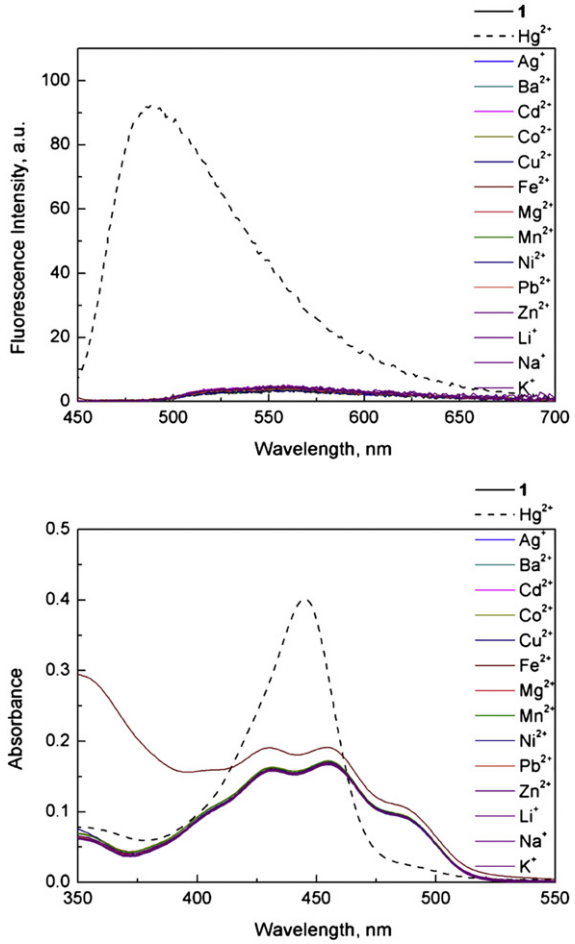

Fig. 2. Absorption (top) and fluorescence (bottom) spectra of **1** in the presence of various metal ions in THF; [M^{n+}]=80 μM, [Hg^{2+}]=40 μM, [**1**]=10 μM, λ_{ex}=445 nm.

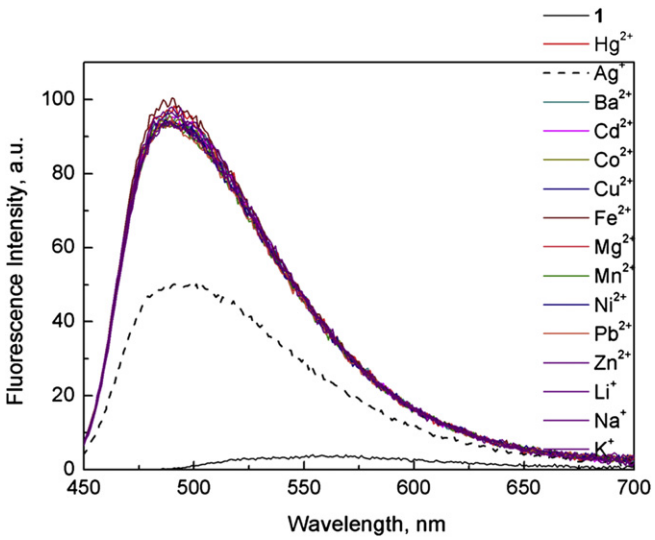

Fig. 3. Fluorescence spectra of **1** in the coexistence of various metal ions and Hg^{2+} in THF; [M^{n+}]=40 μM, [Hg^{2+}]=40 μM, [**1**]=10 μM, λ_{ex}=446 nm.

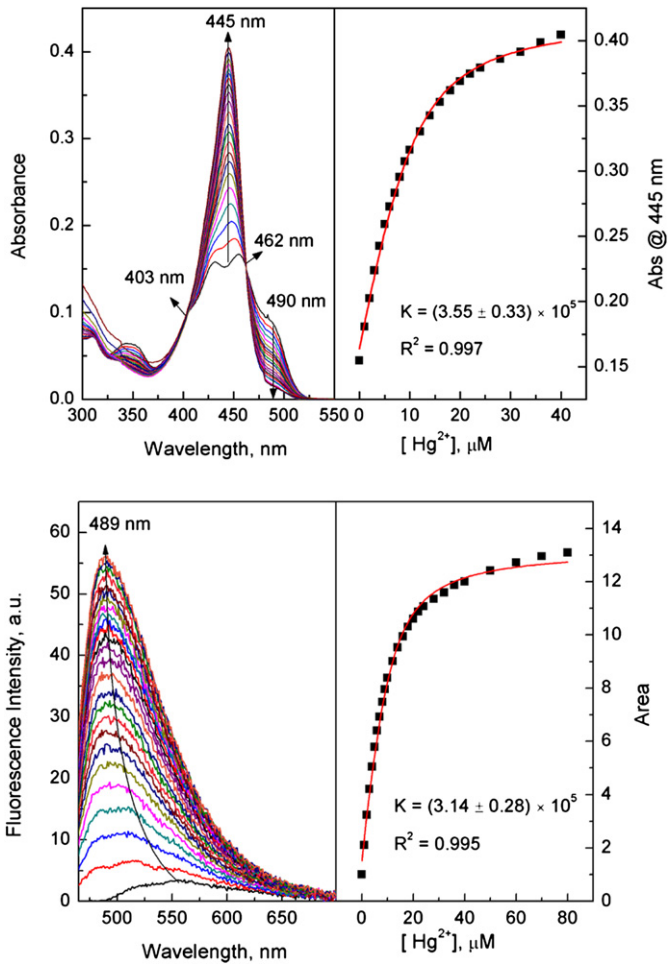

Fig. 4. Absorption (top) and fluorescence (bottom) spectra of **1** in the presence of varying [Hg^{2+}] in THF; [**1**]=10 μM, λ_{ex}=460 nm.

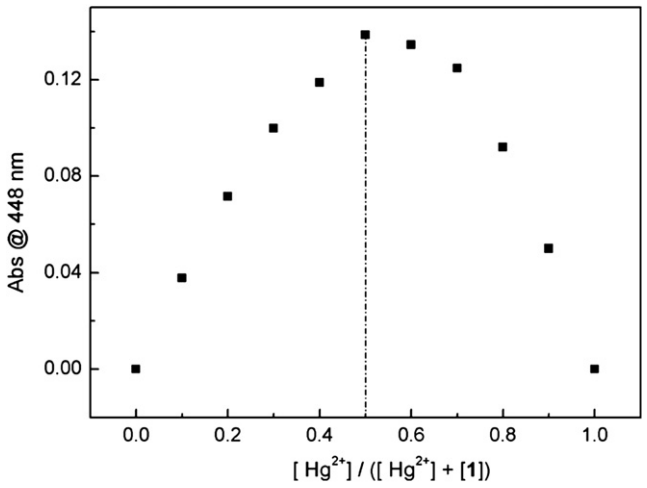

Fig. 5. Job plot for **1**–Hg^{2+} in THF. The total concentration of [Hg^{2+}] and [**1**] is 20 μM.

Intermolecular hydrogen bonding-induced fluorescence enhancement of **1** with quite slight wavelength shift (Fig. 1) and specific Hg^{2+} chelation-promoted fluorescence enhancement with remarkable blue shift (Fig. 2) led us to explore the possibility of ratiometric detection of Hg^{2+} by changing solvent media. We then performed the spectral titration in CH_2Cl_2/MeOH (v/v=9:1). As shown in Fig. 6 (top), the absorption spectra exhibited almost the same behavior as that in THF. With increasing [Hg^{2+}], absorbance of **1** at 489 nm decreased and a new sharp band at 446 nm appeared.

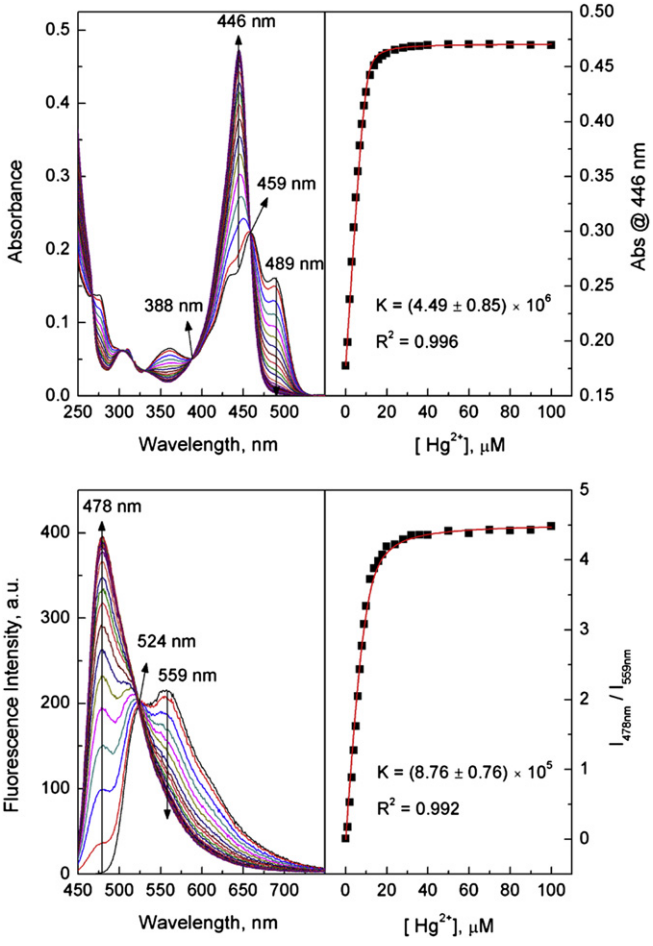

Fig. 6. Absorption (top) and fluorescence (bottom) spectra of **1** in the presence of varying [Hg^{2+}] in CH_2Cl_2/MeOH (v/v=9:1); [**1**]=10 μM, λ_{ex}=446 nm.

It reached an equilibrium more quickly at 2.0 equiv level and the association constant (4.49×10^6 M^{-1}) is improved about one order of magnitude when compared with that in THF. However, the fluorescence behavior was quite different. With increasing [Hg^{2+}], fluorescence intensity at 559 nm decreased, meanwhile a new band at 478 nm enhanced progressively (Fig. 6 bottom) and solution color changed from yellow to cyan under irradiation at 365 nm. An isosbestic emission point was observed at 524 nm. The ratio of the fluorescence intensity at 559 and 478 nm increased linearly with [Hg^{2+}] (0–1.0 equiv). The high association constant (8.76×10^5 M^{-1}) indicated that **1** had a strong binding ability to Hg^{2+} in CH_2Cl_2/MeOH (v/v=9:1).

Reversibility of **1** to Hg^{2+} was examined by the addition of 2 equiv of Br^-/Cl^- to the complex solution in THF (Fig. 7, top and Fig. S2). Immediate fluorescence quenching and solution color change from cyan to dark indicated decomplexation of **1**–Hg^{2+}. The same reversibility was observed in CH_2Cl_2/MeOH (v/v=9:1) (Fig. 7, bottom) where recovery of the fluorescence spectra and solution color was observed after the addition of 2 equiv I^-.

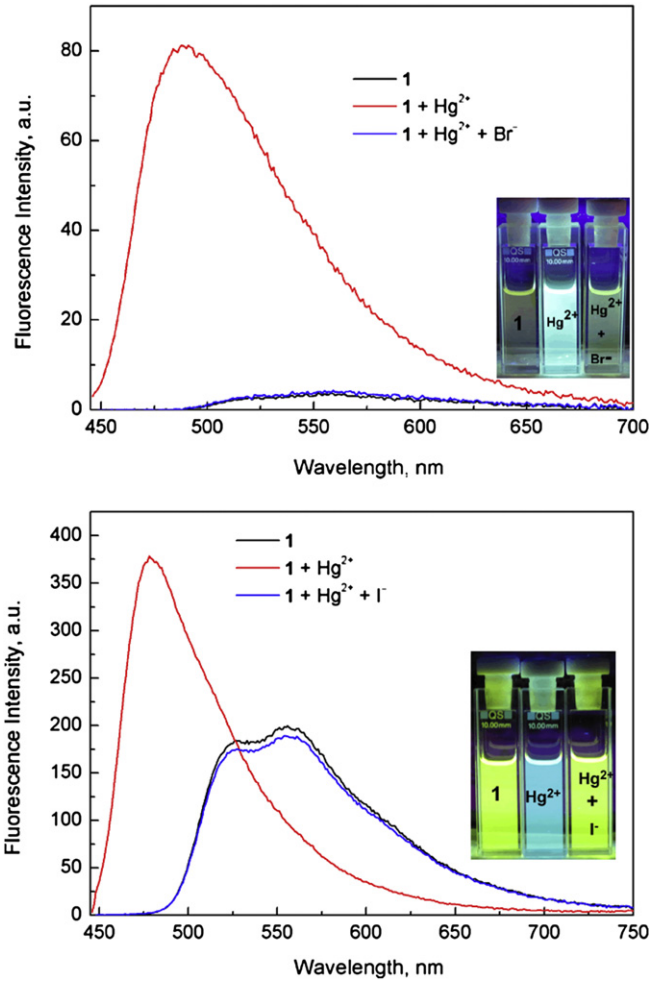

Fig. 7. Fluorescence spectra of **1** in the presence of Hg^{2+}, Hg^{2+} and Br^- in THF (top) or in the presence of Hg^{2+}, Hg^{2+}, and I^- in CH_2Cl_2/MeOH (v/v=9:1) (bottom). [**1**]=10 μM, [Hg^{2+}]=40 μM, [Br^-]=[I^-]=80 μM, λ_{ex}=446 nm.

^{1}H NMR titration in CD_3CN was carried out to examine the binding sites of **1** to Hg^{2+}. By comparing the NMR spectra of **1** (Figs. S8–10) with a known fluorescein methyl ester derivative,[14b] we could assign the signal at 3.6 ppm to methyl group of benzoic moiety while the one at 3.9 ppm to methyl group of xanthene moiety, as confirmed by 2D NMR (HMQC, Fig. S10). The chemical

shifts of protons of the xanthene ring ranged from 6.3 to 7.0 ppm while protons of the benzoic acid moiety from 7.3 to 8.2 ppm. As shown in Fig. 8, upon complexation with Hg^{2+}, all the protons of xanthene moiety shifted downfield dramatically (ca. 0.6–1.0 ppm) while protons of benzoic acid moiety shifted downfield slightly (less than 0.1 ppm), suggesting that the complexation should occur on the xanthene moiety rather than on the benzoic unit. Meanwhile, protons of methyl ether at 3.9 ppm also shifted downfield by 0.2 ppm and spited into two groups while protons of methyl ester at 3.6 ppm were almost not shifted. This fact further supported our assumption that xanthene moiety participated in the complexation process. By analysis of molecular structure of **1**, it is quite obvious that carbonyl group is the binding site for Hg^{2+}. This assumption was further confirmed by investigation of IR spectra of **1** in the presence and absence of Hg^{2+} (Fig. 9). Characteristic carbonyl stretching frequency of the xanthene moiety appeared at 1723 cm^{-1} and bending vibration at 1212 cm^{-1} (the ester carbonyl appeared at 1712 cm^{-1}). In **1**–Hg^{2+} complex, they both downshifted to 1653 and 1184 cm^{-1}, respectively. Time-dependent absorbance of **1** in the presence of Hg^{2+} spectra was also carried out, which showed that the recognition process was immediate (Fig. 10), suggesting a complexation process rather than a chemical reaction since no Hg^{2+}-sensitive chemical function (alkene or alkyne) existed in the structure of **1**. Our results therefore demonstrated that chelation of carbonyl group to Hg^{2+} reduced the electronic density on the xanthene moiety and consequently caused remarkable blue shift of both absorption and fluorescence spectra. Similar to hydrogen bonding interaction, coordination of Hg^{2+} to carbonyl group of xanthene fluorophore might reduce radiationless deactivation of the excited states in organic medium.[16]

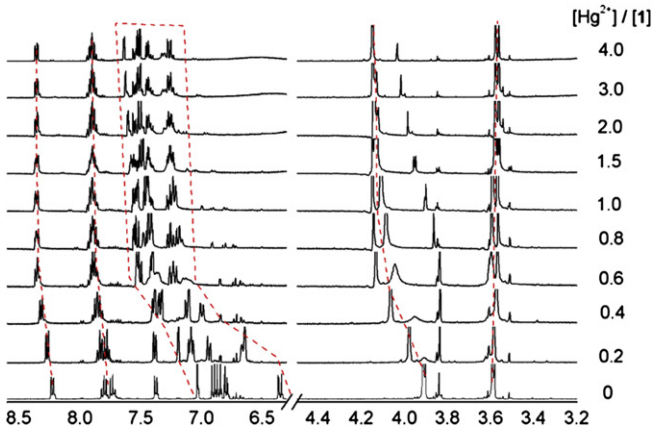

Fig. 8. Partial ^1H NMR spectra of **1** in the presence of varying concentrations of Hg^{2+} in CD_3CN.

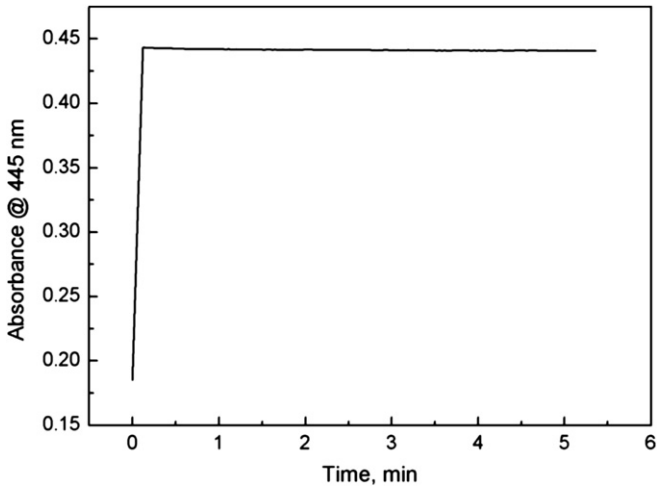

Fig. 10. Time-dependent absorbance of **1** at 445 nm in the presence of 2 equiv of Hg^{2+} in THF.

Compound **2**, where the two methyl groups were replaced by two triazolyl amino esters, was used to investigate how substituent on the xanthene ring affected the binding process of carbonyl to metal ions. Compound **2** showed almost the same photophysical properties as those of **1** including solvatochromism, spectral wavelength and fluorescence quantum yield (Fig. 11, Table 1), indicating that the triazolyl moiety was just a linker and produced no electronic effects on the fluorescent core. Further investigation of its metal ion binding properties showed that introduction of triazolyl group did not affect the selective binding interaction between carbonyl group and Hg^{2+} in THF (Fig. 12 and Fig. S3). Interestingly, spectral titrations of **2** to Hg^{2+} in THF and CH_2Cl_2/MeOH (v/v=9:1) exhibited very similar spectral behavior as that of **1**, such as associate constants (2.94×10^5 M^{-1} in THF (Fig. 13) and 2.26×10^6 M^{-1} in CH_2Cl_2/MeOH (v/v=9:1)) (Fig. 14), binding stoichiometry and reversibility (Figs. S4 to S7). These results together

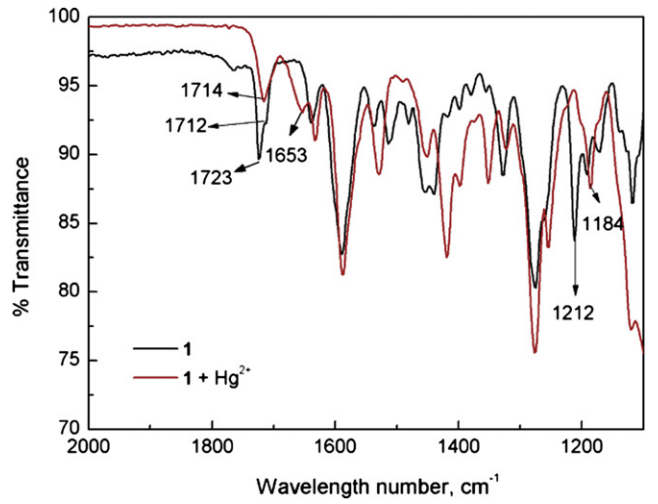

Fig. 9. Partial FTIR of **1** and **1**–Hg^{2+}.

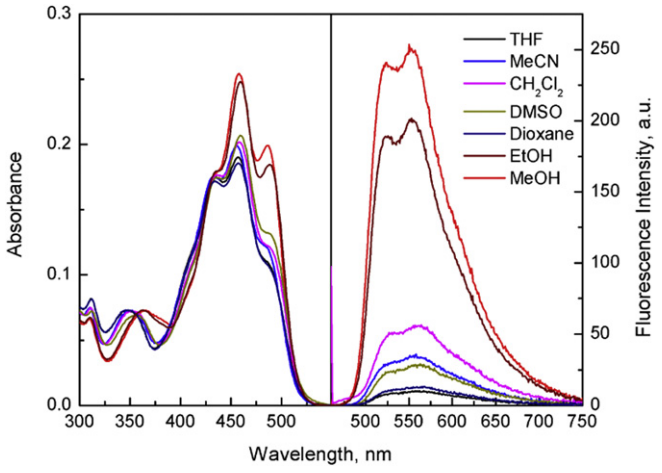

Fig. 11. Absorption (left) and fluorescence (right) spectra of **2** in various solvents; excitation wavelengths correspond to the peaks of absorption band in different solvents, [**2**]=10 μM.

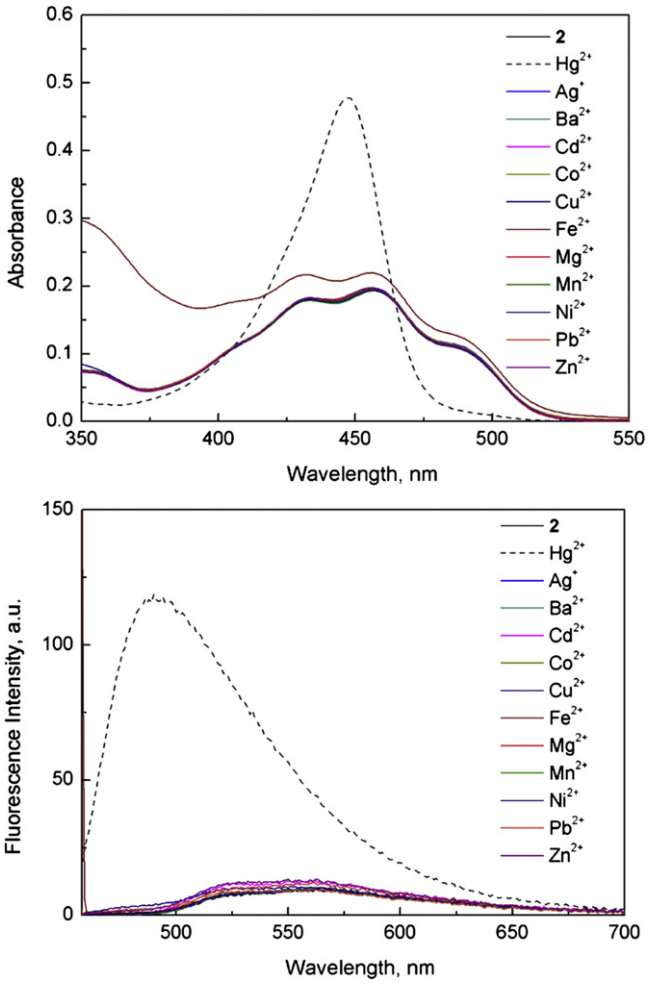

Fig. 12. Absorption (top) and fluorescence (bottom) spectra of **2** in the presence of various metal ions in THF; $[M^{n+}]$=80 μM, $[Hg^{2+}]$=40 μM, [**2**]=10 μM, λ_{ex}=456 nm.

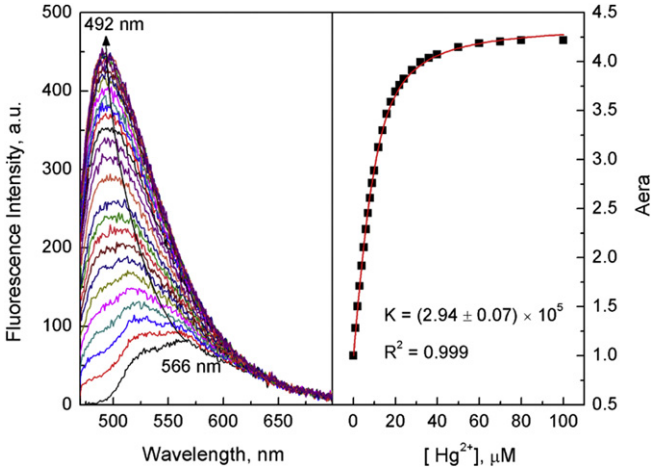

Fig. 13. Fluorescence spectra of **2** in the presence of varying concentrations of Hg^{2+} in THF, [**2**]=10 μM, λ_{ex}=468 nm.

demonstrated that carbonyl group of the xanthenic moiety actually could be a selective binding site for Hg^{2+} and easy accessibility of click reaction might facilitate versatile functionalization on the triazolyl moiety to investigate other sensing approaches, such as FRET.

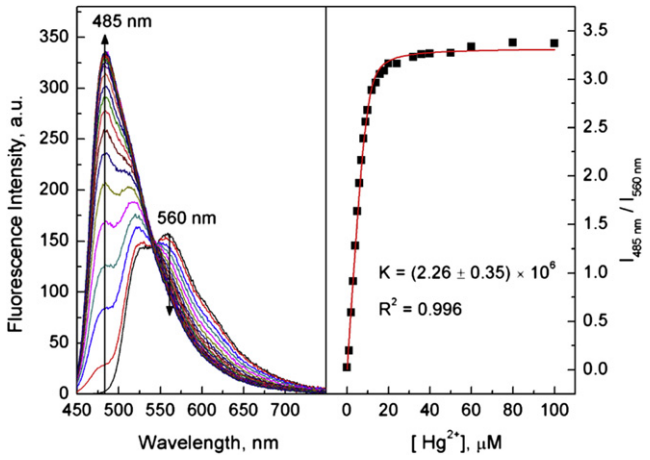

Fig. 14. Fluorescence spectra of **2** in the presence of varying concentrations of Hg^{2+} in CH_2Cl_2/MeOH (v/v=9:1), [**2**]=10 μM, λ_{ex}=447 nm.

3. Conclusions

In summary, we have found that easily synthesized fluorescein derivatives **1** and **2** could be used as highly selective chemosensors for Hg^{2+} over a range of metal ions in THF. In the absence and presence of intermolecular hydrogen bonding interaction, we have developed 'turn-on' fluorescence response to Hg^{2+} in THF and ratiometric detection of Hg^{2+} in CH_2Cl_2/MeOH (v/v=9:1), respectively. ^{1}H NMR titration and IR spectra suggested that specific spectral behavior was due to the complexation between carbonyl group of xanthene moiety and Hg^{2+}. We thus demonstrated how metal coordination, one of most important non-covalent interactions, affected the spectral properties of xanthene fluorophore through direct interaction with its carbonyl group. Furthermore, combination of different non-covalent and/or covalent interactions with carbonyl group may further promote the extensive applications of xanthene dyes in biological and environmental systems.

4. Experimental

4.1. Materials and methods

Absorption spectra were recorded on a Uvikon-940 KON-TRON spectrophotometer and corrected emission spectra were performed on a Jobin-Yvon Spex Fluorolog 1681 spectrofluorometer (1 cm quartz cell was used).

All the solvents were spectroscopic grade and used as received. The tested metal salts included $LiClO_4$, $NaClO_4$, $KClO_4$, $AgNO_3$, $Ba(ClO_4)_2$, $Co(ClO_4)_2$, $Cd(ClO_4)_2$, $Cu(ClO_4)_2$, $Fe(ClO_4)_2$, $Mg(ClO_4)_2$, $Mn(ClO_4)_2$, $Ni(ClO_4)_2$, $Pb(ClO_4)_2$, $Zn(ClO_4)_2$, and $Hg(ClO_4)_2$.

4.2. Spectral measurement

Stock solution of compounds **1** and **2** was prepared in DMSO while metal perchlorate salts in MeCN. For all the spectral tests, concentrations of receptors were fixed at 10 μM. ^{1}H NMR titration was tested in CD_3CN.

4.3. Quantum yield measurement

Fluorescence quantum yield was determined using Coumarin 153 as a standard reference[20] and the quantum yield is calculated using the following equation.

$$\phi_{unk} = \phi_{std}\frac{(I_{unk}/A_{unk})}{(I_{std}/A_{std})}\left(\frac{\eta_{unk}}{\eta_{std}}\right)^2$$

Where ϕ_{unk} and ϕ_{std} are the quantum yield of the sample and standard, I_{unk} and I_{std} are the integrated emission intensity of the corrected spectra of the sample and standard, A_{unk} and A_{std} are the absorbance of the sample and standard at the excitation wavelength (lower than 0.05).

4.4. Determination of association constant

$$Y = Y_0 + \frac{Y_{lim} - Y_0}{2} \times \left\{1 + \frac{C_M}{C_L} + \frac{1}{KC_L} - \left[\left(1 + \frac{C_M}{C_L} + \frac{1}{KC_L}\right)^2 - 4\frac{C_M}{C_L}\right]^{1/2}\right\}$$

Where Y donates the fluorescence intensity or absorbance; C_M and C_L are the concentration of metal ions and ligand; K is the association constant of 1:1 complex. Y_0 and Y_{lim} are the fluorescence intensity or absorbance value when C_M=0 and for full complexation.

Acknowledgements

Y.B.R. thanks the China Scholarship Council (CSC) for support through a scholarship to work at PPSM, ENS Cachan.

Supplementary data

Supplementary data including related spectra data and NMR spectra. Supplementary data associated with this article can be found, in the online version, at doi:10.1016/j.tet.2011.09.028.

References and notes

1. (a) Vallee, B. L.; Ulmer, D. D. *Annu. Rev. Biochem.* **1972**, *41*, 91; (b) Gutknecht, J. *J. Membr. Biol.* **1981**, *61*, 61.
2. Nolan, E. M.; Lippard, S. J. *Chem. Rev.* **2008**, *108*, 3443.
3. (a) Kim, H. N.; Lee, M. H.; Kim, H. J.; Kim, J. S.; Yoon, J. *Chem. Soc. Rev.* **2008**, *37*, 1465; (b) Duong, T. Q.; Kim, J. S. *Chem. Rev.* **2010**, *110*, 6280; (c) Ruan, Y.-B.; Li, A.-F.; Zhao, J.-S.; Shen, J.-S.; Jiang, Y.-B. *Chem. Commun.* **2010**, 4938; (d) Jun, M. E.; Roy, B.; Ahn, K. H. *Chem. Commun.* **2011**, 7583; (e) Cho, Y.-S.; Ahn, K. H. *Tetrahedron Lett.* **2010**, *51*, 3852.
4. Ren, X.; Xu, Q.-H. *Langmuir* **2009**, *25*, 29.
5. (a) Liu, J.; Lu, Y. *Angew. Chem., Int. Ed.* **2007**, *46*, 7587; (b) Zhang, L.; Li, T.; Li, B.; Li, J.; Wang, E. *Chem. Commun.* **2010**, 1476.
6. (a) Li, C.-Y.; Zhang, X.-B.; Qiao, L.; Zhao, Y.; He, C.-M.; Huan, S.-Y.; Lu, L.-M.; Jian, L.-X.; Shen, G.-L.; Yu, R.-Q. *Anal. Chem.* **2009**, *81*, 9993; (b) Tian, M.; Ihmels, H. *Chem. Commun.* **2009**, 3175; (c) Suresh, M.; Mishra, S.; Mishra, S. K.; Suresh, E.; Mandal, A. K.; Shrivastav, A.; Das, A. *Org. Lett.* **2009**, *11*, 2740; (d) Joshi, B. P.; Lohani, C. R.; Lee, K.-H. *Org. Biomol. Chem.* **2010**, *8*, 3220; (e) Santra, M.; Roy, B.; Ahn, K. H. *Org. Lett.* **2011**, *13*, 3422.
7. Gonçalves, M. S. T. *Chem. Rev.* **2009**, *109*, 190.
8. Duan, Y.; Liu, M.; Sun, W.; Wang, M.; Liu, S.; Li, Q. X. *Mini-Rev Org. Chem.* **2009**, *6*, 35.
9. Margulies, D.; Melman, G.; Shanzer, A. *J. Am. Chem. Soc.* **2006**, *128*, 4865.
10. (a) Nolan, E. M.; Lippard, S. J. *Acc. Chem. Res.* **2009**, *42*, 193; (b) Nolan, E. M.; Lippard, S. J. *J. Am. Chem. Soc.* **2003**, *125*, 14270; (c) Nolan, E. M.; Lippard, S. J. *J. Mater. Chem.* **2005**, *15*, 2778; (d) Nolan, E. M.; Racine, M. E.; Lippard, S. J. *Inorg. Chem.* **2006**, *45*, 2742; (e) Nolan, E. M.; Lippard, S. J. *J. Am. Chem. Soc.* **2007**, *129*, 5910; (f) Yoon, S.; Albers, A. E.; Wong, A. P.; Chang, C. J. *J. Am. Chem. Soc.* **2005**, *127*, 16030; (g) Yoon, S.; Miller, E. W.; He, Q.; Do, P. H.; Chang, C. J. *Angew. Chem., Int. Ed.* **2007**, *46*, 6658; (h) Domaille, D. W.; Que, E. L.; Chang, C. J. *Nat. Chem. Biol.* **2008**, *4*, 168; (i) Swamy, K. M. K.; Kim, H. N.; Soh, J. H.; Kim, Y.; Kim, S.-J.; Yoon, J. *Chem. Commun.* **2009**, 1234; (j) Ruan, Y.-B.; Li, C.; Tang, J.; Xie, J. *Chem. Commun.* **2010**, 9220.
11. (a) Jang, Y. J.; Jun, E. J.; Lee, Y. J.; Kim, Y. S.; Kim, J. S.; Yoon, J. *J. Org. Chem.* **2005**, *70*, 9603; (b) Swamy, K. M. K.; Lee, Y. J.; Lee, H. N.; Chun, J.; Kim, Y.; Kim, S.-J.; Yoon, J. *J. Org. Chem.* **2006**, *71*, 8626.
12. McQuade, L. E.; Ma, J.; Lowe, G.; Ghatpande, A.; Gelperin, A.; Lippard, S. J. *Proc. Natl. Acad. Sci. U.S.A.* **2010**, *107*, 8525.
13. (a) Xie, J.; Ménand, M.; Maisonneuve, S.; Métivier, R. *J. Org. Chem.* **2007**, *72*, 5980; (b) Maisonneuve, S.; Fang, Q.; Xie, J. *Tetrahedron* **2008**, *64*, 8716; (c) Ruan, Y. B.; Maisonneuve, S.; Li, C.; Tang, J.; Xie, J. *Front. Chem. China* **2010**, *5*, 208; (d) Ruan, Y. B.; Maisonneuve, S.; Xie, J. *Dyes Pigm.* **2011**, *90*, 239.
14. (a) Zhang, X.-F.; Liu, Q.; Wang, H.; Fu, Z.; Zhang, F. *J. Photochem. Photobiol., A* **2008**, *200*, 307; (b) Guarõn, S. A. P.; Tsang, D.; Skene, W. G. *New J. Chem.* **2007**, *31*, 210.
15. (a) Santra, M.; Ryu, D.; Chatterjee, A.; Ko, S.-K.; Shin, I.; Ahn, K. H. *Chem. Commun.* **2009**, 2115; (b) Santra, M.; Ko, S.-K.; Shin, I.; Ahn, K. H. *Chem. Commun.* **2010**, 3964; (c) Chen, X.; Ko, S.-K.; Kim, M. J.; Shin, I.; Yoon, J. *Chem. Commun.* **2010**, 2751; (d) Taki, M.; Iyoshi, S.; Ojida, A.; Hamachi, I.; Yamamoto, Y. *J. Am. Chem. Soc.* **2010**, *132*, 5938; (e) Garner, A. L.; St Croix, C. M.; Pitt, B. R.; Leikauf, G. D.; Ando, S.; Koide, K. *Nat. Chem.* **2009**, *1*, 316; (f) Garner, A. L.; Koide, K. *J. Am. Chem. Soc.* **2008**, *130*, 16472; (g) Garner, A. L.; Song, F.; Koide, K. *J. Am. Chem. Soc.* **2009**, *131*, 5163; (h) Garner, A. L.; Koide, K. *Chem. Commun.* **2009**, 86; (i) Song, F.; Watanabe, S.; Floreancig, P. E.; Koide, K. *J. Am. Chem. Soc.* **2008**, *130*, 16460.
16. Martin, M. M. *Chem. Phys. Lett.* **1975**, *35*, 105.
17. Miura, T.; Urano, Y.; Tanaka, K.; Nagano, T.; Ohkubo, K.; Fukuzumi, S. *J. Am. Chem. Soc.* **2003**, *125*, 8666.
18. Li, C.; Tang, J.; Xie, J. *Tetrahedron* **2009**, *65*, 2395.
19. (a) Avirah, R. R.; Jyothish, K.; Ramaiah, D. *Org. Lett.* **2007**, *9*, 121; (b) Avirah, R. R. Synthesis and Study of Photophysical And Metal Ion Binding Properties of a Few Novel Semisquaraine and Croconaine Dyes. Ph.D. Dissertation, Cochin University of Science and Technology, 2010.
20. Grabolle, M.; Spieles, M.; Lesnyak, V.; Gaponik, N.; Eychmuller, A.; Resch-Genger, U. *Anal. Chem.* **2009**, *81*, 6285.